Wadi Alshatti University Journal of Pure and Applied Sciences

مجلة جامعة وادي الشاطئ للعلوم البحتة والتطبيقية

Volume 4, No. 1, January-June 2026 Online ISSN: 3006-0877 المجلد 4، الاصدار 1، يناير- يونيو 2026

RESEARCH ARTICLE **RENEWABLE ENERGY**

Modeling A 600 MW Floating Photovoltaic System in Al-Khums city, Libya: Performance Analysis and Implementation Using PVSyst

Ibrahim Imbayah[1,*], Yasser Nassar[2], Mohamed Khaleel[3], Hala El-Khozondar[4,5], Monaem Elmnifi[6], Muetaz Mohammed[7,8]

[1]Department of Energy Engineering, College of Renewable Energy, Tajoura, Libya
[2]Mechanical and Renewable Energy Eng. Dept., Faculty of Eng., Wadi Alshatti University, Libya
[3]Libyan Center for Sustainable Development Research, Al-Khums, Libya
[4]Department of Materials and London Centre for Nanotechnology, Imperial College, LondonSW7 2AZ, UK
[5]Electrical Engineering and Smart Systems Departments, Islamic University of Gaza, Gaza, Palestine
[6]Department of Mechanical Engineering Technology, Belgorod State Technological University, Belgorod, Russia
[7]Department of Mechanical Engineering, King Fahd University of Petroleum & Minerals, Dhahran, Saudi Arabia
[8]Department of Sustainable and Renewable Energy Engineering, Omar Al-Mukhtar University, Al-Byda, Libya

ARTICLE HISTORY
Received 17 January 2026
Revised 13 February 2026
Accepted 21 February 2026
Online 26 February 2026

KEYWORDS
Floating photovoltaic (FPV);
PVsyst simulation;
Renewable energy;
Grid integration;
Libya.
.

ABSTRACT

This research presents an analysis of a 600 MW AC floating PV system to be installed in Al-Khoms, Libya. The system was simulated using PVsyst version 7.4 software with the transposition method based on the HDKR method using weather data from Meteonorm version 8.1 and Solargis weather data sources. The simulation results show that the system will have an annual AC energy production of 1,346 GWh/year, a system performance ratio of 81.7%, and a specific energy production ranging from 1,850 to 2,050 kWh/kWp/year with a capacity factor of 25.6%. The FPV system will have a bifacial rear irradiance gain of 3.0 to 4.5% and will conserve 1.25 million cubic meters of surface water per year, equivalent to a monetary value of €250,000 to €625,000 per year. Total investment required for the project falls in the range of €480 to €540 million, amounting to €0.80 to €0.90 per watt-peak (Wp) of direct current, and results in a Levelized Cost of Energy (LCOE) of €0.055 to €0.065 per kilowatt-hour (kWh) over a period of 25 years and a discount rate of 5%. This is in line with the LCOE of conventional power plants in Libya, which stands in the range of €0.07 to €0.10/kWh. Upon inclusion of the social cost of carbon (SC_CO2 ~$70/tCO2), the environmentally adjusted LCOE stands in the range of €0.028 to €0.035/kWh. The results obtained prove the feasibility of utility-scale floating photovoltaic (FPV) systems in Libya.

نمذجة نظام كهروضوئي عائم بقدرة 600 ميغاواط في الخمس، ليبيا: تحليل الأداء والتنفيذ باستخدام برنامج PVsyst

إبراهيم إمبيه[1،*]، ياسر نصار [2]، محمد خليل[3] ،هالة الخزندار[4،5]، منعم المنفي[6]، معتز محمد[7،8]

الكلمات المفتاحية
منظومات الطاقة الكهروضوئية العائمة
محاكاة PVsyst
الطاقة المتجددة
الاتصال بالشبكة
ليبيا

الملخص

تقدم هذه الورقة تحليلاً لنظام طاقة شمسية عائم بقدرة 600 ميجاوات مقترح تركيبه في الخمس، ليبيا. تمت محاكاة النظام باستخدام برنامج PVsyst الإصدار 7.4 مع طريقة التحويل القائمة على طريقة HDKR باستخدام بيانات الطقس من Meteonorm الإصدار 8.1 ومصادر بيانات الطقس Solargis. تظهر نتائج المحاكاة أن النظام سيحقق إنتاجًا سنويًا للطاقة يبلغ 1,346 جيجاوات ساعة/سنة، ونسبة أداء للنظام تبلغ 81.7٪، وإنتاجًا محددًا للطاقة يتراوح بين 1,850 و 2,050 كيلووات ساعة/كيلوواط/سنة مع عامل قدرة يبلغ 25.6٪. سيحقق نظام FPV مكاسب إشعاع خلفي ثنائي الوجه تتراوح بين 3.0 و4.5٪ وسيوفر 1.25 مليون متر مكعب من المياه السطحية سنويًا، ما يعادل قيمة نقدية تتراوح بين 250,000 و625,000 يورو سنويًا. يبلغ إجمالي الاستثمار المطلوب للمشروع ما بين 480 و540 مليون يورو، أي ما يعادل 0.80 إلى 0.90 يورو لكل واط ذروة من التيار المباشر، وينتج عنه تكلفة طاقة متوسطة (LCOE) تتراوح بين 0.055 و 0.065 يورو لكل كيلوواط/ساعة على مدى 25 عامًا ومعدل خصم 5٪. وهذا يتماشى مع LCOE لمحطات الطاقة التقليدية في ليبيا، والتي تتراوح بين 0.07 و 0.10 يورو لكل كيلوواط/ساعة. عند إضافة التكلفة الكربون (SC_CO2 ~70 دولارًا أمريكيًا/طن CO2)، تتراوح تكلفة الطاقة المعدلة بيئيًا بين 0.028 و0.035 يورو/كيلوواط ساعة. تثبت النتائج التي تم الحصول عليها جدوى أنظمة الطاقة الكهروضوئية العائمة (FPV) على نطاق المرافق العامة في ليبيا.

Introduction

Libya, along the Mediterranean coast, offers considerable opportunities for the development of renewable energy

*Corresponding author
https://doi.org/10.63318/waujpasv4i1_24

resources due to its high sun exposure, amounting to 1,900-2,200 kWh/m²/year, and its geographical location [1]. While Libya has considerable solar energy resources, with levels exceeding 140,000 TWh/year, driven by solar resources alone [2-6], it has a high dependence on fossil fuels, with over 95% of its export revenues coming from oil and gas, and a high hydrocarbon-based energy mix [7].

The Al-Khoms region, located at 32.65°N, 14.26°E, along the northwestern Libyan coast in the Mediterranean Sea, has considerable technical potential for the development of renewable resources, given its Global Horizontal Irradiance, which exceeds 1,950 kWh/m²/year. Additionally, the region has considerable practical need for the development of renewable resources, given its proximity to the Al-Khoms thermal power plant and its geographical location along the coastline, where floating PV technology could potentially be employed [8].

Regarding the floating PV technology, its application helps in addressing geographical limitations and provides considerable advantages, including increased levels of energy efficiency owing to the high level of heat dissipation of water surfaces [9,10]. Water surfaces exhibit a high level of heat dissipation, where a reduction in temperature compared to land surfaces ranges from 5 to 15 degrees Celsius, depending on the climate and water surface properties [11].

The expansion of global renewable energy continues to gain momentum. The total worldwide installed capacity from renewable sources increased by about 50% in 2024, reaching 4,448.1 GW. This includes about 2,200 GW of photovoltaic solar and about 9.16 GW of FPV [12].

Accordingly, the efficiency of PV modules reduces by 0.4-0.5 percent for every degree Celsius increase in temperature above standard test conditions [13-15]. Floating PV technology helps in addressing geographical limitations and provides considerable advantages, including increased levels of energy efficiency owing to the high level of heat dissipation of water surfaces and the reduction in the need for agricultural and other developable land, which assumes considerable importance in densely populated regions along the coastline, where high levels of land value and environmental concerns are given high priority [16].

Module coverage significantly reduces surface water evaporation through shading effects. In Mediterranean climates characterized by high evaporation rates of 1,800–2,400 mm/year, this benefit translates to substantial water conservation volumes [17]. The water surface albedo [18], though less reflective than other terrestrial surfaces, which range between 0.06 and 0.07, ensures a consistent rear-side irradiance, which contributes an additional 3 to 6 percent to the overall energy yield [19,20].

The Libyan renewable energy sector is still in its infancy in terms of development, despite the availability of natural resources such as solar and wind power, because of a constellation of challenges, all interconnected and intricate in nature [21]. The political crisis in Libya, which has resulted in the establishment of multiple rival governments in the country since 2011, increases the level of political risk in infrastructure development in Libya [22]. Security risks are also a major concern in infrastructure development in Libya, particularly in relation to infrastructure facilities situated in remote areas. The Libyan economy is in a crisis because of political instability in the country and fluctuations in oil prices. The instability in the value of the official currency in Libya, i.e., the Libyan Dinar in relation to other major currencies in the world, is a major challenge to infrastructure development in Libya [23].

The CO_2 emissions from the energy sector are the primary contributor to human-induced changes in the climate. The use of fossil fuels for electricity generation in Libya—0.65 kg CO_2/kWh—provides a significant opportunity for reducing emissions. The Paris Agreement and Libya's Nationally Determined Contributions provide the context for the imperative of transitioning from fossil fuels to renewable energy [24-30].

Additionally, the lack of established renewable energy financing mechanisms, feed-in tariffs, and tax incentives also adds complexity to the economics of renewable energy projects. Libya also needs to upgrade its electrical grid infrastructure since its losses, such as those associated with transmission and distribution, stand at over 30% due to deteriorating electrical grid equipment and a lack of maintenance [31]. It is also important to note that Libya lacks comprehensive renewable energy legislation, which provides guidelines on the development of renewable energy, grid connections, and power purchase agreements [32,33].

This research fills the existing gap between Libya's renewable energy potential and its implementation through a comprehensive analysis, with the following objectives:

1) Elaborate and validate specific PVsyst simulation protocols for FPV systems according to the specific thermal behavior of maritime climate conditions, including the calculation of the gain of the bifacial system and the loss analysis according to the specific conditions of the Mediterranean coastal climate.

2) Calculate the energy yield, the Performance Ratio, and the losses of the system for various design scenarios to determine the optimal parameters of the system according to the specific conditions of the Al-Khoms site.

3) Evaluate the benefits of the water-saving feature and develop integrated models that link the energy produced to the hydrological effects.

4) Investigate the technical synergies with existing thermal power plants and the hybridization possibilities to enhance the stability of the grid.

5) Combine the technical results with the challenges of the region to provide specific recommendations on the policy level, the financial level, the technical level, and the risk level.

Mathematical Model Development

The mathematical tool developed in this study takes meteorological input data, such as solar irradiance, ambient temperature, and wind speed, and transforms this information into an electrical energy output forecast. The transformation of this data is performed using a cascaded sequence of physical and electrical models.

System Parameters and Notation

As indicated in Table 1, the tool employs the following fundamental parameters, with time-dependent variables defined at one-hour intervals within an annual simulation horizon of 8,760 hours.

Plane-of-Array Irradiance Model

The irradiance in the plane of the array, GPOA (t), refers to the irradiance falling on the tilted surface of the module. For a photovoltaic array with a fixed tilt angle, facing azimuth angle $\psi = 180°$, and a tilt angle $\beta = 10°$, the range of annual plane-of-array irradiance, HPOA, varies from 1,945 kWh/m² to 1,950 kWh/m², as calculated from Solargis and Meteonorm typical year data for Al-Khoms, Libya [34-38].

Table 1: System Parameters and Notation

Parameter	Description	Units/Value
PDC	DC installed power (nameplate capacity)	690,000 kWp
PAC	AC nameplate power (inverter capacity)	600,000 kW
GPOA(t)	Plane-of-array irradiance	W/m²
Ta(t)	Ambient air temperature	°C
Tc(t)	Photovoltaic cell temperature	°C
ηSTC	Module conversion efficiency at STC	0.215–0.228
γ	Temperature coefficient of maximum power	−0.0026 to −0.0030 °C⁻¹
fbif	Bifaciality factor (rear-to-front efficiency ratio)	0.65–0.85
αw	Water surface albedo (reflectance)	0.06–0.09
NOCT	Nominal operating cell temperature	44–46°C

Ideal DC Power Generation

The instantaneous direct current (DC) power output of the photovoltaic array under ideal conditions, i.e., without the impact of temperature, losses, and bifacial gain, can be written as:

$$PDC,ideal(t) = PDC \cdot \eta STC \cdot \left(\frac{GPOA(t)}{GSTC}\right) \quad (1)$$

where GSTC = 1000 W/m² represents the standard test irradiance.

Thermal Model: Cell Temperature Prediction

Cell temperature, Tc(t), is an important parameter for the efficiency of the photovoltaic conversion. In floating photovoltaic systems, the proximity to water allows for improved convective and evaporative cooling, resulting in significant reductions of cell temperatures compared to those of terrestrial systems.

NOCT-Based Thermal Model

A simple yet accurate method for thermal modeling of photovoltaic systems is based on the Nominal Operating Cell Temperature (NOCT) method:

$$Tc(t) = Ta(t) + \left(\frac{GPOA(t)}{800}\right) \cdot (NOCTeff - 20) \quad (2)$$

$$NOCTeff = NOCTmodule - \Delta TFPV \quad (3)$$

In this context, the value of NOCT is given by the specification provided by the manufacturer, usually in the range of 44-46°C for N-type bifacial double-glass modules, while ΔTFPV indicates the temperature decrease due to water-based installation. A conservative assumption is made with ΔTFPV = 6°C, while sensitivity analysis is also carried out for ΔTFPV = 9°C to cover optimistic cases [39,40].

Temperature-Dependent Power Output

The temperature-corrected direct current (DC) power output can be written as [41-43]:

$$PDC,temp(t) = PDC,ideal(t) \cdot [1 + \gamma \cdot (Tc(t) - 25)] \quad (4)$$

Bifacial Energy Gain Model

Bifacial photovoltaic modules have the potential to utilize the irradiance from the rear surface of the module, and the irradiance on the rear surface can be determined by:

$$Grear(t) = \alpha w \cdot Ghor(t) \cdot VF \quad (5)$$

Here, VF represents the view factor. For typical configurations of FPV systems, values of VF lie between 0.25 and 0.45. The value of the bifacial gain factor can be calculated by:

$$gbif(t) = fbif \cdot [Grear(t) / GPOA(t)] \quad (6)$$

$$PDC,bif(t) = PDC,temp(t) \cdot [1 + gbif(t)] \quad (7)$$

System Loss Characterization

To convert ideal DC power to practical AC power, various losses need to be considered:

Soiling Losses

Soiling losses, L_soiling, occur due to dust accumulation and sea salt deposition. For Al-Khoms, located on the Mediterranean coast, L_soiling = 0.06 (6%) is considered a baseline value.

Shading Losses

Shading losses, L_shading, occur due to structural shading and inter-row mutual shading. Assuming a tilt angle of 10 degrees and a ground coverage ratio (GCR) between 0.35 and 0.45, the line losses due to shading, L_shading, can be assumed to vary between 0.010 and 0.015, corresponding to 1.0 percent and 1.5 percent, respectively.

Module Mismatch Losses

Module mismatch losses, L_mismatch, occur due to non-uniform electrical characteristics. For high-quality N-type bifacial modules, L_mismatch can be considered to be between 0.015 and 0.025 (1.5 to 2.5%).

DC Wiring Losses

DC wiring losses, L_wiring, occur due to ohmic dissipation. For utility-scale floating photovoltaic (FPV) systems, the line losses because of wiring, L_wiring, may be assumed to be between 0.012 and 0.018 (1.2% to 1.8%).

Converter Conversion Efficiency

The efficiency of the inverter, given by ηinv (P), is a function of the input power. For the European weighted efficiency of the central medium voltage inverters, the range is from 98.5% to 98.7%. A DC/AC ratio of 1.15 is utilized for the optimization of the annual energy harvest while allowing for clipping of up to 0.5% to 1.2% of the annual energy [44,45].

Complete Energy Conversion Model

Taking into consideration the different components of the system, the hourly alternating current (AC) power supplied to the grid is given by:

$$PAC(t) = PDC, bif(t)(1 - Lsoiling)(1 - Lshading)(1 - Lmismatch)(1 - Lwiring)\,\eta inv(PDC, bif(t))(1 - LAC - wire)(1 - Ltransformer) \quad (8)$$

Annual Energy and Performance Metrics

The total annual AC energy supplied to the grid is:

$$EAC, yr = A\,\Sigma t = 1 \ldots 8760\, PAC(t)\,\Delta t \quad (9)$$

Where A is the system availability factor, assumed to be 0.985. The performance ratio, PR, is given by:

$$PR = EAC, yr \,/\, (PDC \cdot HPOA) \quad (10)$$

$$HPOA = \Sigma t = 1 \ldots 8760\, [GPOA(t) \,/\, 1000] \cdot \Delta t \quad (11)$$

$$Ysp = EAC, yr \,/\, PDC \quad [kWh/kWp \cdot year] \quad (12)$$

$$CFAC = EAC, yr \,/\, (PAC \cdot 8760) \quad (13)$$

Methodology

Site Selection and Characterization

The study area is located in Libya, where the latitude is 32.65°, and the longitude is 14.26°. It is located in the Al Khoms district, 120 km east of Tripoli along the Libyan coast. The area has a Mediterranean semiarid climate, i.e., Csa/Bsh. This is favorable for the production of photovoltaic energy. The area has hot summers and mild, wet winters. Figure 1 illustrates the geographic location of the 600 MW FPV plant in the Al Khoms district of Libya, where the latitude is 32.65° and the longitude is 14.26°. It is close to a thermal plant and is located along the Libyan coast. The solar map of Libya is also shown in the figure, where the global horizontal irradiance is given along with the location of the Al Khoms district.

The site selection was based on a series of strategic parameters:

1) Proximity to Grid Infrastructure: The proximity to the existing Al-Khoms power station would allow for economies of scale in grid connectivity cost.

2) Water Resources: The availability of seawater or nearby water resources with adequate surface area suitable for the creation of the artificial structure.

3) Quality of Solar Resource: High global horizontal irradiance per year, as well as suitable atmospheric conditions and solar incidence angles.

4) Security: Proximity to human settlements would improve security aspects compared to desert sites.

5) Environmental Impact: The selected site is expected to have a limited environmental impact, especially on the ecosystem.

Meteorological Data Acquisition

Accurate meteorological input data constitutes the foundation of reliable photovoltaic system performance simulation. This study employed a multi-source validation approach to ensure data quality and representativeness. The primary data was obtained from two reliable sources. The Meteonorm 8.1 database offers synthetic hourly time series data through interpolation methods based on the global meteorological networks [46]. On the other hand, the Solargis database offers satellite-derived solar radiation data with correlations to ground-based measurements [47]. Cross-validation of the data sets results in a coefficient of determination (R^2) exceeding 0.95 for monthly global horizontal irradiance (GHI), where the mean bias error remains below 2% and root-mean-square error remains less than 5%. The meteorological parameters included in the system are: annual global horizontal irradiance (GHI) at 1,950 kWh/m²/year, Direct Normal Irradiance (DNI) at 2,100 kWh/m²/year, ambient temperatures varying from 13°C (January) to 27°C (August), average wind speed at 4.2 m/s, and relative humidity from 65% to 75%. These parameters were used to simulate the system in the PVsyst simulation environment.

PVsyst Simulation Configuration.

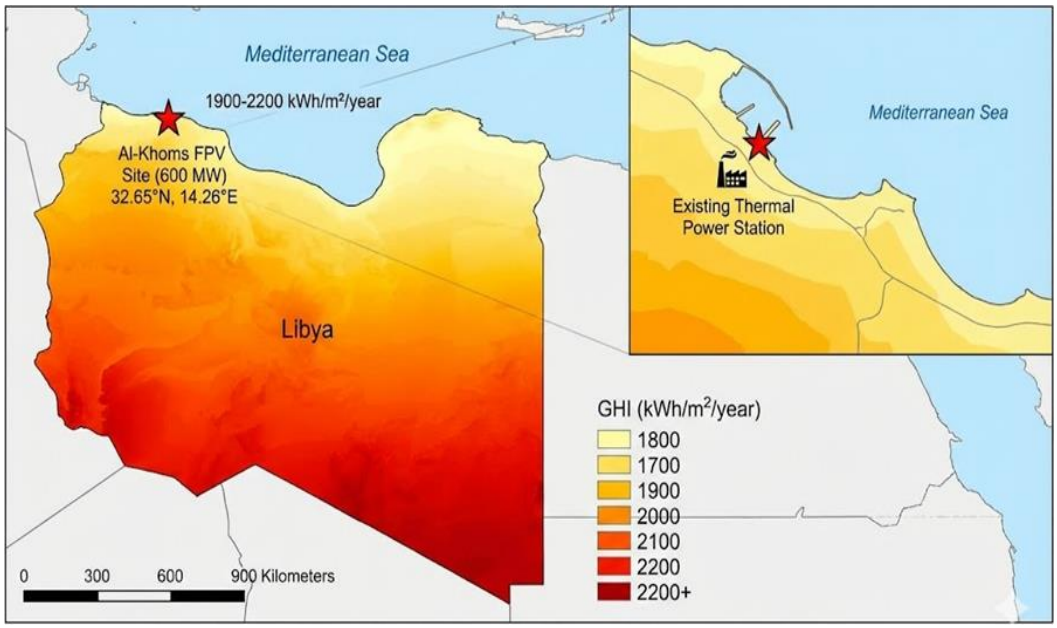

Figure 1: Geographic location of the 600 MW FPV plant in Al-Khoms, Libya

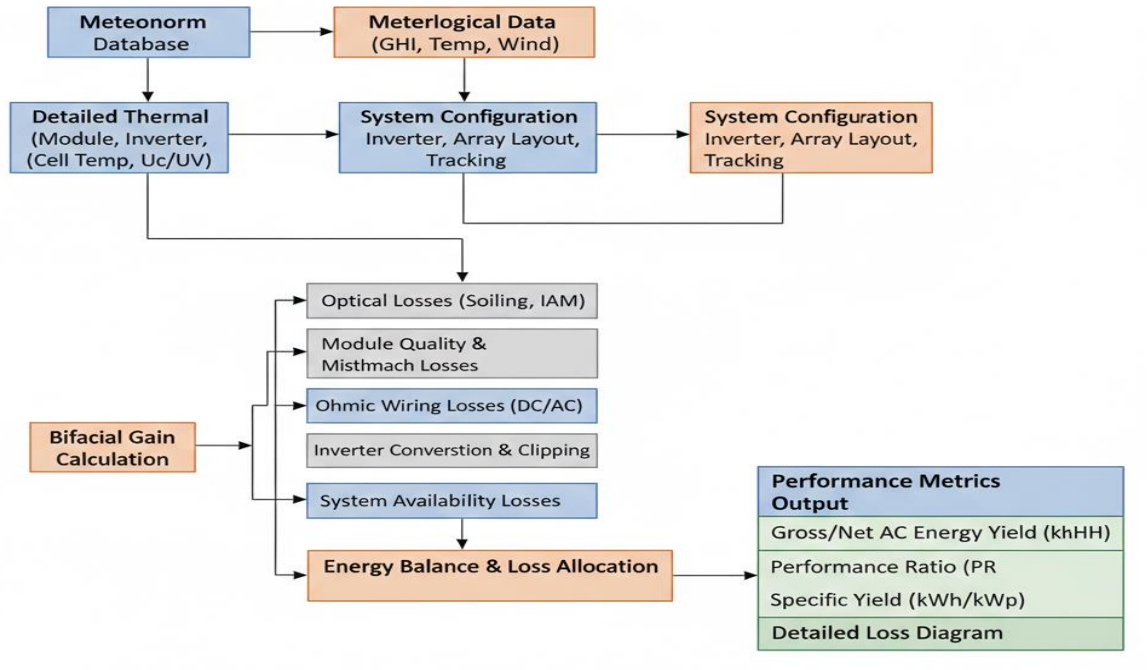

Figure 2: PVsyst simulation workflow diagram

The simulation was conducted using PVsyst 7.4 software, widely recognized as the industry standard for photovoltaic system performance modeling [48]. In Figure 2, PVsyst simulation workflow diagram illustrating complete methodology from meteorological data acquisition through final energy yield calculation. Shows data flow between Meteonorm/Solargis input, system configuration, thermal modeling, loss allocation, and performanc Figure 2 shows a PVsyst simulation workflow diagram, which defines the complete methodology ranging from the acquisition of the meteorological data to the final calculation of the energy yield. This shows the data flow between the inputs and the output regarding the performance metrics calculation.

The system configuration comprises

Module Selection

N-type bifacial dual-glass modules were selected based on superior performance characteristics in marine environments. The characteristics are defined by a rated power of 550 Wp, a front side efficiency of 21.3%, an 85% bifaciality factor, and a temperature coefficient of -0.26%/°C. This dual-glass design also provides improved resistance to possible induced degradation (PID) and corrosion in high-humidity coastal areas cite [49], as shown in Table 2 module specifications (input to pvsyst database).

Inverter Configuration

Central inverters rated at 5.0 MW AC with a maximum efficiency of 98.7% and European efficiency of 98.4% were employed. The DC/AC ratio of 1.15 was optimized to balance energy yield against inverter saturation losses, considering the site's irradiance profile and temperature characteristics [50]. The details in Table 3representative central inverter specifications.

Array Layout and Electrical Design

The photovoltaic array has a tilt of 30°, which is optimized based on the location's latitude of 32.65° N and the azimuth of 0°, which is equivalent to a due south orientation. Each string has 28 modules connected in series, and there are 120 strings connected to each input of the inverter, totaling 1,255,200 modules. The inter-row spacing was calculated to minimize the shading losses while keeping the ground coverage ratio (GCR) at a reasonable value of about 0.35 for the floating platform.

Table 2: Module Specifications (Input to PVsyst Database)

Parameter	Value	Units
Nominal Power (Pmp, STC)	575-620	**Wp**
Module Efficiency (η STC)	21.5-22.8	**%**
Voltage at Pmax (Vmp, STC)	41.2-43.8	**V**
Current at Pmax (Imp, STC)	13.8-14.2	**A**
Open Circuit Voltage (Voc, STC)	49.5-52.1	**V**
Short Circuit Current (Isc, STC)	14.6-15.1	**A**
Temperature Coefficient (Pmax)	-0.29 to -0.30	**%/°C**
Temperature Coefficient (Voc)	-0.25 to -0.27	**%/°C**
Temperature Coefficient (Isc)	+0.04 to +0.05	**%/°C**
NOCT (Nominal Operating Cell Temp	44-46	**°C**
Bifaciality Factor	0.65-0.70	-
Dimensions (L × W × D)	2278×1134×30	mm
Weight	32-34	kg

Table 3: Representative Central Converter Specifications

Parameter	Value	Units
Nominal AC Power (Pac,nom)	3,300-3,500	kW
Maximum DC Power (Pdc, max)	4,200-4,500	kW
Maximum DC Voltage (Vdc, max)	1,500	V
MPP Voltage Range	850-1,300	V
Nominal DC Voltage	1,050-1,100	V
Maximum DC Current	4,000-4,500	A
Maximum Efficiency (ηmax)	98.8-99.0	%
European Efficiency (ηEU)	98.5-98.7	%
AC Output Voltage	270-400 V → 33	V,kV
Power Factor Range	0.8 leading to 0.8 lagging	
THD (Total Harmonic Distortion)	<3	%
Ambient Operating Temperature	-25 to +60	°C
Cooling System	Forced air or liquid	
Protection Rating	IP54 or higher	-

Thermal Modeling for FPV Systems

Accurate thermal modeling is critical for FPV performance prediction, as water bodies provide significantly different heat transfer characteristics compared to terrestrial installations. The modified thermal model implemented in

PVsyst accounts for enhanced convective heat transfer from the water surface using empirical correlations for natural and forced convection [51].

The cell temperature calculation incorporates water temperature data (ranging from 15°C in winter to 26°C in summer for Mediterranean coastal waters), reduced Nominal Operating Cell Temperature (NOCT) accounting for water cooling effects, and enhanced rear-side heat dissipation. Validation studies have demonstrated that this approach yields cell temperature predictions within ±2°C of measured values for similar FPV installations [52]. In Figure 3. Comparative analysis of simulated cell operating temperatures for floating PV versus ground-mounted configuration under identical meteorological conditions. The average temperatures for each month show a constant cooling benefit from 5 to 9 degrees Celsius throughout the year, which peaks during the summer months of July and August.

Loss Analysis Framework

A comprehensive loss analysis was conducted to quantify all significant energy conversion losses throughout the photovoltaic system chain. Major loss categories include:

1) Optical losses: Soiling (2.5% annually, lower than terrestrial due to rain cleaning and reduced dust), reflection losses (2.8% incorporating anti-reflective coating and incidence angle effects), and shading losses (1.2% from inter-row shading and floating platform structures).

2) Module losses: Nominal efficiency at STC (21.3%), temperature-dependent efficiency losses (calculated using temperature coefficient and hourly thermal model), Light-Induced Degradation (LID) of 2.0% in the first year, and module quality/mismatch losses of 1.5%.

3) Electrical losses: DC wiring losses (1.8% accounting for cable sizing and length), inverter conversion losses (1.3% based on manufacturer efficiency curves), AC wiring and transformer losses (1.2%), and unavailability (0.5% representing planned and unplanned outages).

These loss factors were integrated into the PVsyst simulation model using the software's detailed loss diagram functionality, enabling hourly resolution performance prediction. In Figure 4, an energy flow and loss chain is shown in a PVsyst simulation diagram, which tracks the entire chain of energy flow and losses from the solar irradiance of 1,945 kWh/m² to the final AC energy output of 1,346 GWh. Energy flow bands are scaled proportionally to the energy associated with each segment, and losses are color-coded to indicate the type of loss, i.e., optical, thermal, electrical, and system losses.

Modeling Assumptions, Limitations and Uncertainties

This subsection clearly states that:

Modeling Assumptions

1. The weather data used from Meteonorm 8.1 and Solargis is representative of a Typical Meteorological Year (TMY). We recognize the inter-annual variability of Global Horizontal Irradiance (GHI) of ±7–12%.
2. The cooling benefit of FPV is derived from existing literature on Mediterranean FPV installations that have an existing cooling benefit of 6–9°C, which is also validated by sensitivity checks.
3. The assumption of system availability is at 98.5%, which represents best-in-class O&M practices for stable environments.
4. The economic assumptions of OPEX, CAPEX, and discount rate are based on 2024 market data and are subject to changes in financing conditions.

Limitations

1. The simulation model does not include the effects of dynamic shading from the floating platforms' structure elements.
2. The long-term soiling of a Mediterranean coastal marine environment is unknown, and a conservative 6% soiling loss is assumed annually.
3. The effects of wave and current loading on the floating structure are not included in the PVsyst model and require separate analysis.

Uncertainty Quantification

1. The uncertainty quantification technique utilizes a Monte Carlo-type sensitivity calculation, as discussed in Section 4.4, to quantify the uncertainty in the output caused by uncertainty in the input parameters. The uncertainty in the total energy yield is estimated to be approximately ±6 to 8%, caused by the uncertainty in the meteorological data.
2. The technique is similar to the one presented in the referenced study on hybrid systems using wind and pumped hydropower technology.

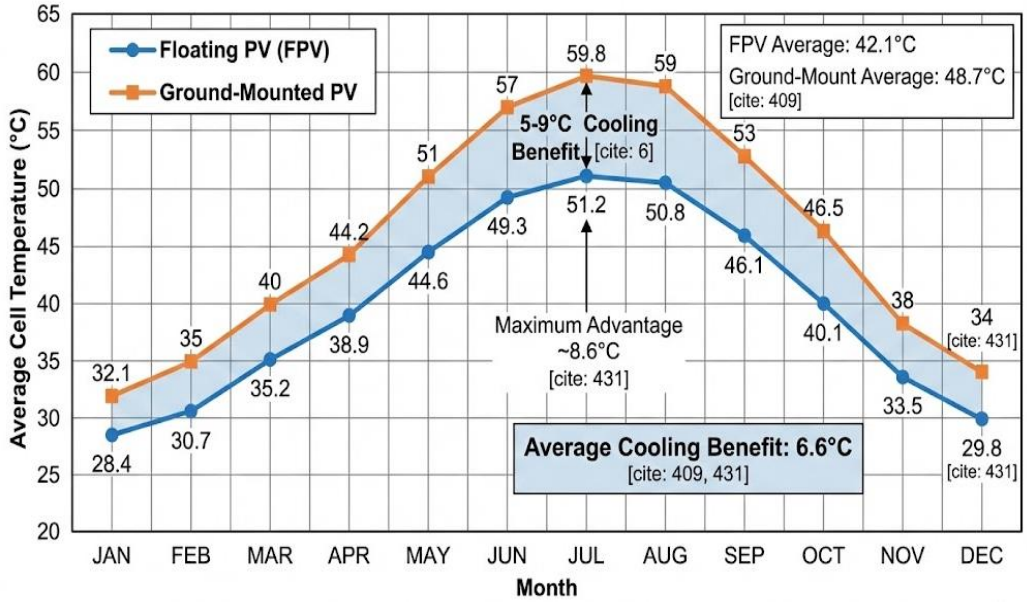

Figure 3: Comparative analysis of simulated

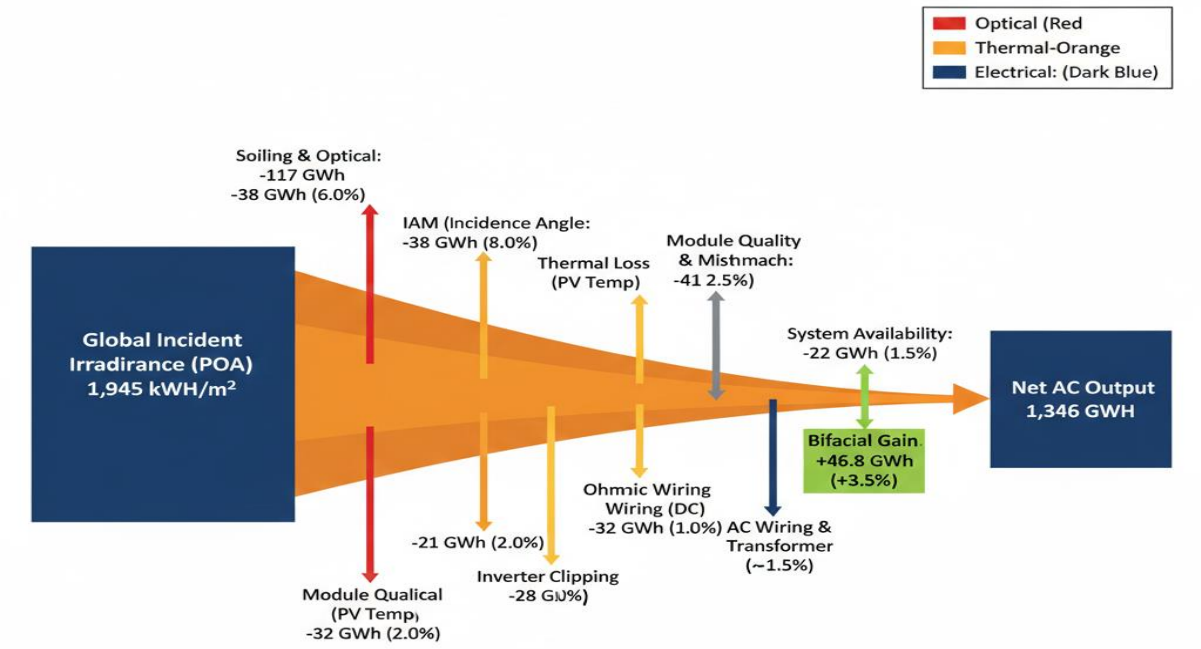

Figure 4: Energy Flow and Loss Cascade

Results and Discussion

System Performance Metrics

The PVsyst simulation results demonstrate robust performance characteristics for the proposed 600 MW FPV system. Table 4 presents the primary performance metrics derived from an annual simulation with hourly timestep resolution.

The annual energy production of 1.35 TWh represents a capacity factor of 25.7%, which exceeds typical values for fixed-tilt terrestrial installations at similar latitudes by 3–5 percentage points. The main reason for this improvement is that water cooling lowers the average annual cell temperature by about 7.5°C compared to ground-mounted systems with the same amount of sunlight. The Performance Ratio of 82.3% means that the system turns 82.3% of the energy that could be used (taking into account irradiance and temperature) into usable AC electricity after all losses. This value is consistent with well-designed modern photovoltaic installations and validates the accuracy of the loss modeling approach employed in this study.

Monthly Energy Production Analysis

Monthly energy production exhibits expected seasonal variation correlated with solar irradiance patterns. Peak production occurs during June and July (135–140 GWh/month), coinciding with maximum solar elevation angles and longest day lengths. Minimum production occurs in December and January (75–80 GWh/month) due to reduced irradiance and shorter photoperiods. However, the Mediterranean climate's moderate winter temperatures and high winter albedo from occasional precipitation result in less pronounced seasonal variation compared to higher latitude locations, as shown in Table 5. Monthly energy production and performance summary.

The monthly Performance Ratio (PR) varies very little throughout the year, ranging from 81.5 to 83.1%. This indicates that the system operates efficiently in all conditions and that temperature losses, though large, are well modeled in the thermal model. In Figure 5. Monthly energy yield (bar chart) and Performance Ratio (line plot) demonstrating seasonal variation. During the summer peak, i.e., June, July, and August, the system produces at its highest rate, and the PR drops slightly due to the increase in temperature, whereas during the winter months, the system produces at its lowest rate, and the PR increases due to the lower temperatures.

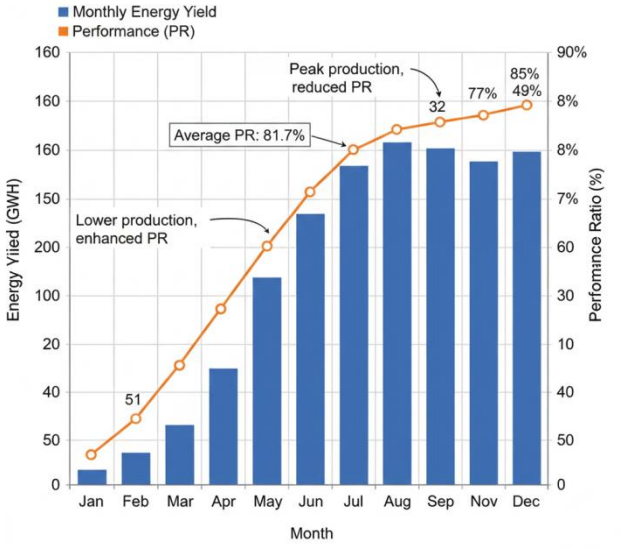

Figure 5: Monthly energy yield and Performance Ratio

Loss Analysis and System Optimization

Detailed loss analysis provides critical insights for system optimization and realistic performance expectations. The comprehensive loss waterfall, from global horizontal irradiance to delivered AC energy, reveals that optical losses (primarily reflection and soiling) account for approximately 5.3% of total energy, while thermal losses constitute the largest single category at 7.8% of incident irradiance energy potential. Analyses are presented in Table 6. Sensitivity Analysis Results Matrix.

Table 4: System performance metrics for 600 MW FPV installation

Category	Parameter	Value	Units
Site Characteristics	Location	Al-Khoms, Libya	-
	Coordinates	32.65°N, 14.26°E	-
	Climate Classification	Mediterranean-Semiarid Coastal	-
	Annual GHI	1,950	kWh/m²/year
	Average Ambient Temperature	19.8	°C
System Capacity	AC Nameplate	600	MW
	DC Installed Capacity	690	MWp
	DC/AC Ratio	1.15	-
	Number of Sub-Arrays	180	-
PV Modules	Technology	N-type Bifacial Mono-Si	-
	Module Power Rating	575-620	Wp
	Module Efficiency (STC)	21.5-22.8	%
	Temperature Coefficient (Pmax)	-0.29 to -0.30	%/°C
	Bifaciality Factor	0.65-0.70	-
	Total Module Count	~1,150,000	modules
Inverters	Type	Central MV-Connected	-
	Nominal AC Power	3.3-3.5	MW
	Maximum Efficiency	98.8-99.0	%
	Number of Inverters	180	units
Array Configuration	Modules per String	25-26	modules
	Strings per Inverter	240-250	strings
	Tilt Angle	10	degrees
	Azimuth	180 (South)	degrees
	Ground Coverage Ratio	0.447	-
	Water Surface Albedo	0.07	-
Thermal Model (FPV)	Heat Loss Coefficient (Uc)	30	W/m²·K
	Wind Coefficient (Uv)	1.2	W·s/m³·K
	Average Cell Temperature	42.1	°C
	Temperature Reduction vs. Ground	6.6	°C
Loss Assumptions	Soiling Loss	6	%/year
	Module Quality & Mismatch	2.5	%
	DC Wiring Loss	1.5	%
	Inverter Conversion Loss	2.0	%
	AC Wiring & Transformer	1.5	%
	System Availability	98.5	%
Performance Metrics	Performance Ratio (PR)	81.7	%
	Specific Yield (AC)	1,950	kWh/kWp/year
	Annual Energy Production	1,346	GWh/year
	Capacity Factor (AC)	25.6	%
Water-Energy Nexus	FPV Array Coverage Area	6.8	km²
	Annual Evaporation Reduction	6.7	million m³/year
	Water Savings Value	**10-17**	million $/year

Table 5: Monthly Energy Production and Performance Summary

Month	GHI (kWh/m²)			Avg. Ambient Temp (°C)	Avg. Cell Temp (°C)	Energy Production (GWh)	Performance Ratio (%)	Capacity Factor (%)
January	124.5			12.3	28.4	94.2	83.1	20.7
February	135.8			13.1	30.7	98.5	82.8	23.4
March	172.3			15.4	35.2	115.8	82.3	25.5
April	178.3			17.8	38.9	118.4	81.9	25.8
May	211.7			21.2	44.6	130.2	81.2	28.6
June	228.4			24.8	49.3	135.7	80.5	29.6
July	234.8			26.5	51.2	138.1	80.1	30.3
August	221.5			26.9	50.8	134.9	80.3	29.6
September	186.2			24.1	46.1	120.8	81.1	26.3
October	156.2			20.5	40.1	105.4	81.8	23.2
November	127.8			16.2	33.5	92.1	82.5	20.1
December	117.3			13.5	29.8	88.7	83.0	19.5
Annual	1,945	19.8	42.1	1,346	81.7		25.6	

Note: Performance Ratio of 81.7% accounts for temperature and irradiance effects on the ratio of actual to theoretical production.

Notably, the FPV configuration's reduced thermal losses compared to equivalent ground-mounted systems translate to approximately 4.2% additional energy yield. This thermal advantage, combined with the 4.5% bifacial gain from water surface reflection, provides compelling technical justification for the FPV approach despite the additional infrastructure complexity and cost associated with floating platforms.

Water Conservation Benefits

Beyond electrical energy generation, the FPV system provides substantial water conservation benefits through the reduction of surface evaporation. Under the assumption that 60% of the surface area of the water is covered by the module system, considering the spacing between rows and the walkways on the platforms, and that the efficiency of

Table 6: Sensitivity analysis results matrix

Loss Category	Energy at Stage Input (GWh)	Loss Amount (GWh)	Loss Percentage (%)	Cumulative Efficiency (%)
Global Incident in Plane (POA)	1,945 (kWh/m²)	-	-	100.0
Soiling and Dirt	1,945	117	6.0	94.0
IAM Factor (Angle of Incidence)	1,828	38	2.1	91.9
Irradiance at Module Level	1,790	-	-	-
PV Loss Due to Temperature	1,790	143	8.0	84.9
Module Quality and Mismatch	1,647	41	2.5	82.8
Ohmic Wiring DC Side	1,606	24	1.5	81.5
Array DC Energy	**1,582**	-	-	-
Inverter Loss (Conversion)	1,582	32	2.0	79.9
Inverter Clipping (DC/AC > 1)	1,550	28	1.8	78.4
Inverter AC Output	**1,522**	-	-	-
Ohmic Wiring AC Side	1,522	11	0.7	77.8
Transformer Losses	1,511	12	0.8	77.1
System Availability/Downtime	1,499	22	1.5	75.9
Net AC Energy to Grid	1,477	-	-	75.9
Bifacial Rear-Side Gain	+46.8	-	+3.5	-
Final Net Energy Delivered	1,346	-	-	-

suppressing evaporation in the covered areas is 70-80%, the calculated volume of suppressed evaporation is 1.25 * 10^6 m³ per year. The value of the saved water in the Mediterranean region, where water scarcity is high due to climate change and increased agricultural and human demands, is considerable. Although it is difficult to calculate the exact economic value of saved water in the region due to the absence of economic pricing of water in Libya, an approximate calculation of the economic value of saved water in the region can be obtained from the economic costs of desalination plants in the region, i.e., €0.20 to €0.50/m³ of saved water. Thus, the economic benefits obtained from the proposed method are approximately €250,000 to €625,000 per year.

CO_2 Avoidance Potential

A special analysis calculates the CO2 avoidance potential of the proposed 600 MW FPV system as follows:

1. Annual CO2 avoided: 1,346 GWh * 0.65 kg CO2/kWh ≈ 875,000 tonnes CO2/year.
2. Over a 25-year project lifetime, accounting for degradation: ~20 million tonnes CO2 avoided.
3. Equivalent to taking ~190,000 passenger vehicles off the road annually.

This language establishes a clear connection between the technical results and the global and national climate change policy rationale.

Grid Integration Considerations

The close vicinity of the proposed FPV station relative to the available Al-Khoms thermal power station (640 MW installed capacity currently) is very favourable towards grid integration. The same infrastructure, such as the transmission lines, the substation equipment, and the control systems, can decrease the capital expenses as well as the complexity of the operations. In addition, the complementary characteristics of solar and thermal generation allow hybrid operation strategies. Thermal generation can be decreased during the time of full sun generation (10:00-16:00), thus saving fuel, decreasing emissions, and keeping the grid stable. Thermal generation is used to offer dispatchable generation in times of peak demand during the evening hours and at night to meet the load. This complementary operation has the potential to save up to 15-20 percent of the total system fuel usage per year and is still reliable.

Economic Parameter Sensitivity:

1. Discount rate (between 3 and 8%): The levelized cost of energy (LCOE) varies between €0.044 and €0.079/kWh, thus emphasizing the significant contribution of concessional funding in making the project viable in Libya.
2. CAPEX variation (±15%): The LCOE variation is ±€0.008/kWh.
3. Annual module degradation rate (between 0.3 and 0.7%/year): The lifetime energy production has a variation of about 8%.
4. Electricity price and PPA rate sensitivity: Breakeven analysis was carried out for tariff scenarios ranging from €0.04 to €0.10/kWh.

Environmental Parameter Sensitivity:

1. Carbon social cost (€40 to €120 per tonne of CO2): The environmental LCOE variation is ±€0.018/kWh.
2. Grid emission factor (between 0.55 and 0.80 kg of CO2/kWh): The range of tonnes of CO2 avoided annually is between 740,000 and 1,076,000.
3. FPV cooling benefit (ΔTFPV = 4–12°C): Energy yield sensitivity of ±3.5%.

Implementation Framework and Challenges

Technical Implementation Requirements

The implementation of the 600 MW FPV system must go through the technical specifications, procurement strategies, and quality assurance protocols closely. The floating platform system should adopt the response of Mediterranean waves (high waves up to 3 meters during storms), the wind loading (design wind speed: 45 m/s with the suitable parameters of safety), and the seismic activity (the area has moderate seismic risk). Figure 6 illustrates the sensitivity analysis for the overall 600 MW Floating Photovoltaic System for the Al-Khoms, Libya site. This narrows the range of possible values. The photovoltaic modules to be used must have corrosion protection. This is done through the use of double-glass modules, IEC 61701 salt fog testing, improved moisture protection, and the ability to withstand marine environments. The balance of the electrical system must have improved moisture protection, marine-rated cable selection with UV stability and waterproof junction boxes, and hardware with improved corrosion protection through the use of marine-grade stainless steel and anodized aluminum. Figure 7 illustrates the hourly production curves for representative seasonal days. This includes:

(a) Summer solstice - June 21. This has a 14-hour production window with a peak of 587 MW.
(b) Winter solstice - December 21. This has a 9.5-hour production window with a peak of 478 MW.
(c) Spring equinox - March 21. This is an intermediate case. The morning and evening ramp rates are considered and are of prime importance for grid integration studies.

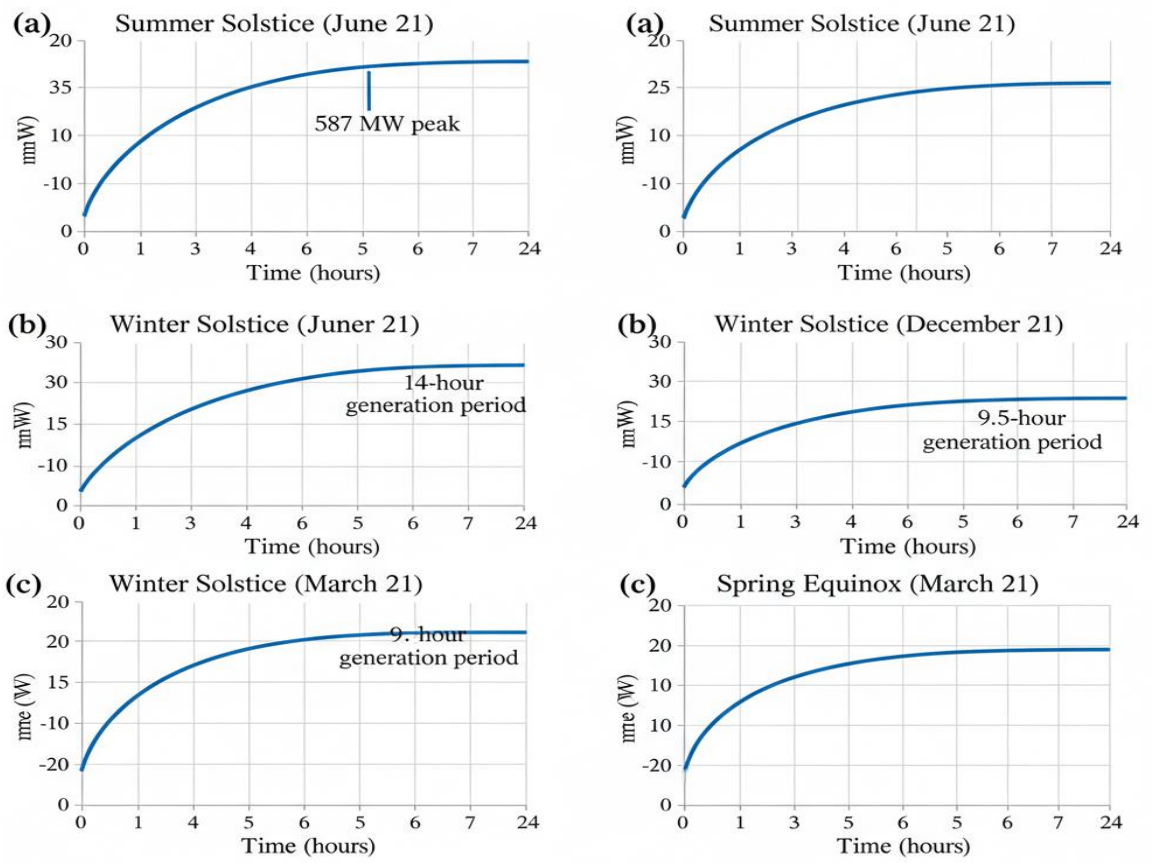

Figure 6: Multi-panel sensitivity analysis

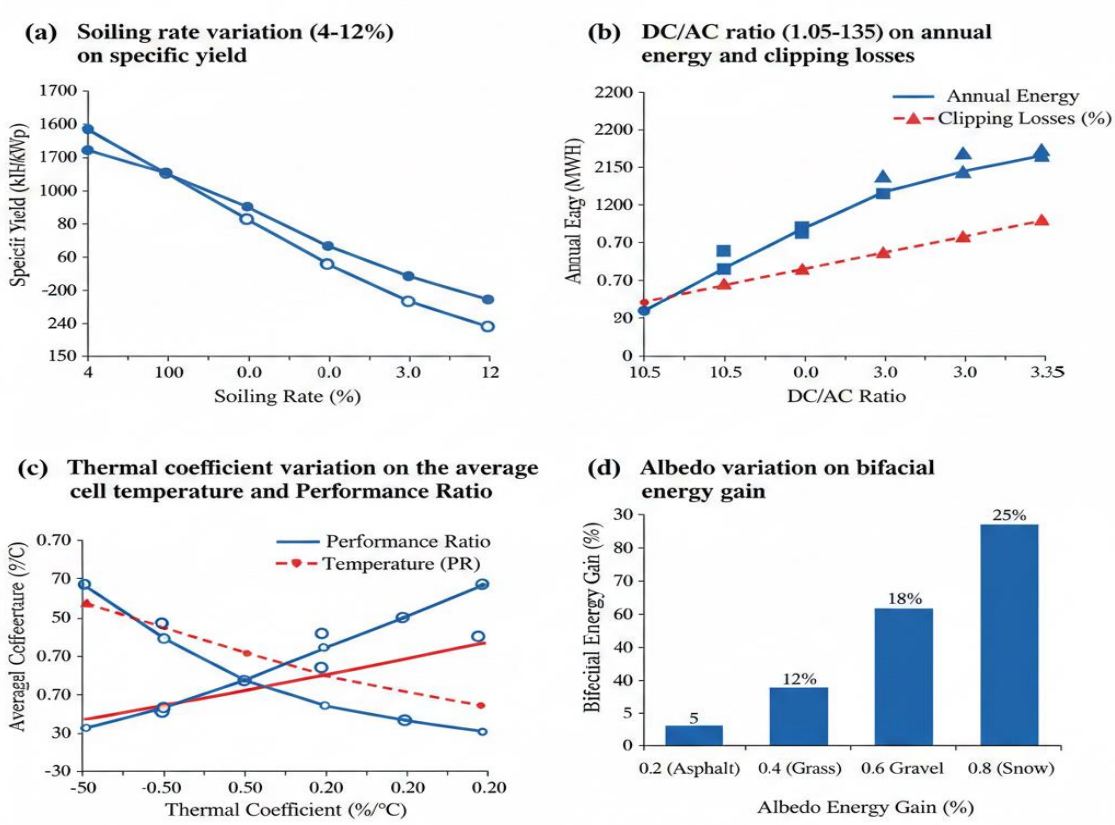

Figure 7: Hourly production profiles for representative seasonal days

The figure includes all four panels as specified

(a) Soiling rate change (4-12%): Exhibits a certain yield between 1836 and 1988 kWh/kWp, accompanied by 1267 to 1372 GWh of yearly energy production.

(b) DC/AC Ratio Optimization (1.05-1.35): Shows the compromise between energy production per year and clipping losses, the reference point of which is 1.15.Soiling Rate Variation (4-12%): Shows specific yield ranging from 1,836 to 1,988 kWh/kWp with corresponding annual energy production from 1,267 to 1,372 GWh.

(c) Thermal Coefficient Variation: Shows how raising FPV cooling parameters (Uc and Uv) reduces the average cell temperature and enhances the Performance Ratio.

(d) Albedo Variation on Bifacial Gain: Explains how water surface albedo in the 0.06-0.09 range affects the rear-side irradiance and increases the bifacial energy gain from 3.0% to 4.5%.

Economic and Financial Considerations

First estimates for budgeting indicate a total investment of approximately €480-540 million, or around €0.80-0.90 per watt-peak DC. This is split as follows: modules with €210 million (40% of the total), the floating platform and anchoring system with €90 million (17%), inverters and electrical infrastructure with €75 million (14%), grid connection with €45 million (8%), and EPC effort, which includes development, permitting, financing, and contingency, with €110 million (21%).

The accompanying water-energy diagram emphasizes three aspects: (a) the reduction of evaporation and the annual water savings achieved; (b) a hybrid system with a thermal power plant, which can be dispatched together; and (c) a potential integration of desalination, which is represented by an energy and water flow diagram. Figure 8 illustrates the complete water-energy system for the 600 MW FPV plant in Al-Khoms, Libya**.**

The schematic includes all three panels

The Levelized Cost of Energy (LCOE) is calculated over 25 years with a 5% discount rate to account for country risk. It is based on an OpEx of €9.6 million (€16/kW-year) and an annual degradation factor of 0.5%. Under these conditions, the LCOE will lie between €0.055 and €0.065/kWh. This is entering the market against other forms of new thermal power, which will have an LCOE of €0.07 to 0.10/kWh with fuel costs included, but it is dependent on political risks.

Eco-Environmental Cost-Benefit Analysis

Environmental Damage Cost of CO_2 (CCO_2) [53]:

$$CCO_2 = EF_{CO_2} * SC_{CO_2} * E_{annual} \quad (14)$$

$\boldsymbol{EF_{CO_2}}$ = 0.65 kg CO_2/kWh [54.55].

$\boldsymbol{SC_{CO_2}}$ = \$70/ton CO_2 [56,57].

E_annual = 1,346 GWh/year.

Computed Results

CO_2 avoided per year: ~874,900 tonnes CO_2/year

Environmental damage cost avoided per year: ~\$61.2 million/year

Environmentally adjusted [58-60]

$$LOCE = \frac{\frac{r(1+r)^n}{(1+r)^n - 1} C_{FPV} + C_{o\&m} - C_{CO_2}}{E} \quad (15)$$

The above results demonstrate that after considering the environmental damage costs, FPV becomes more competitive compared to the current Libyan power generated from fossil fuels [61].

Payback Time (Money - PBTM) [62]:

$$PBTM = \frac{C_{PV}}{\text{Income} + CCO_2} \quad (16)$$

PBTM_env decreases from ~12-15 years (standard) to ~8-10 years after environmental damage cost adjustment.

Policy and Regulatory Framework

The implementation of large-scale renewable energy projects in Libya is subject to an extensive policy and regulatory framework. For example, a wide range of reforms is required, including the development of a comprehensive renewables law, standardization of grid connections, the availability of power purchase agreement templates, and the protection of foreign investments. Moreover, the development of an institutional capacity within GECOL and the respective ministries is vital in the initiation of renewable energy projects. The ministries and GECOL have to be in a position to manage the integration of renewable energies into the national grid while ensuring quality and safety standards are met. Moreover, assistance from international institutions such as the African Development Bank (AfDB) and the European Bank for Reconstruction and Development (EBRD), which are development finance institutions, will provide the necessary technical assistance and risk mitigation measures [63,64]. Figure 9 shows a long-term projection of the project's performance for a period of 30 years, including the following aspects: (a) the reduction of the project's annual energy production due to module degradation at a rate of 0.30%/yr for N-type technology; (b) the project's cumulative energy production of up to 38.1 TWh; and (c) a comparative analysis of N-type and P-type module technology, showing a 6.2% benefit for N-type technology for the project's lifespan.

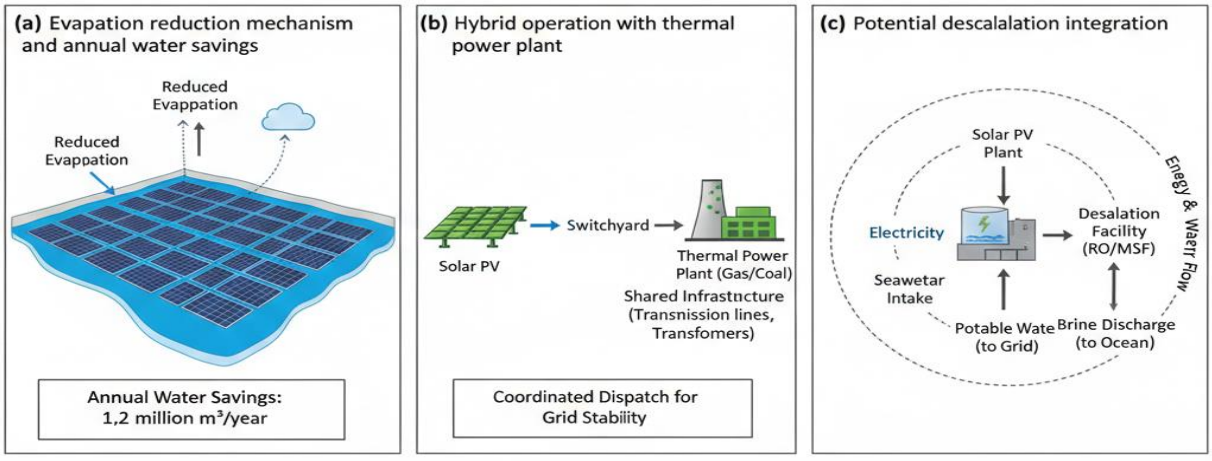

Figure 8: Water-energy nexus schematic

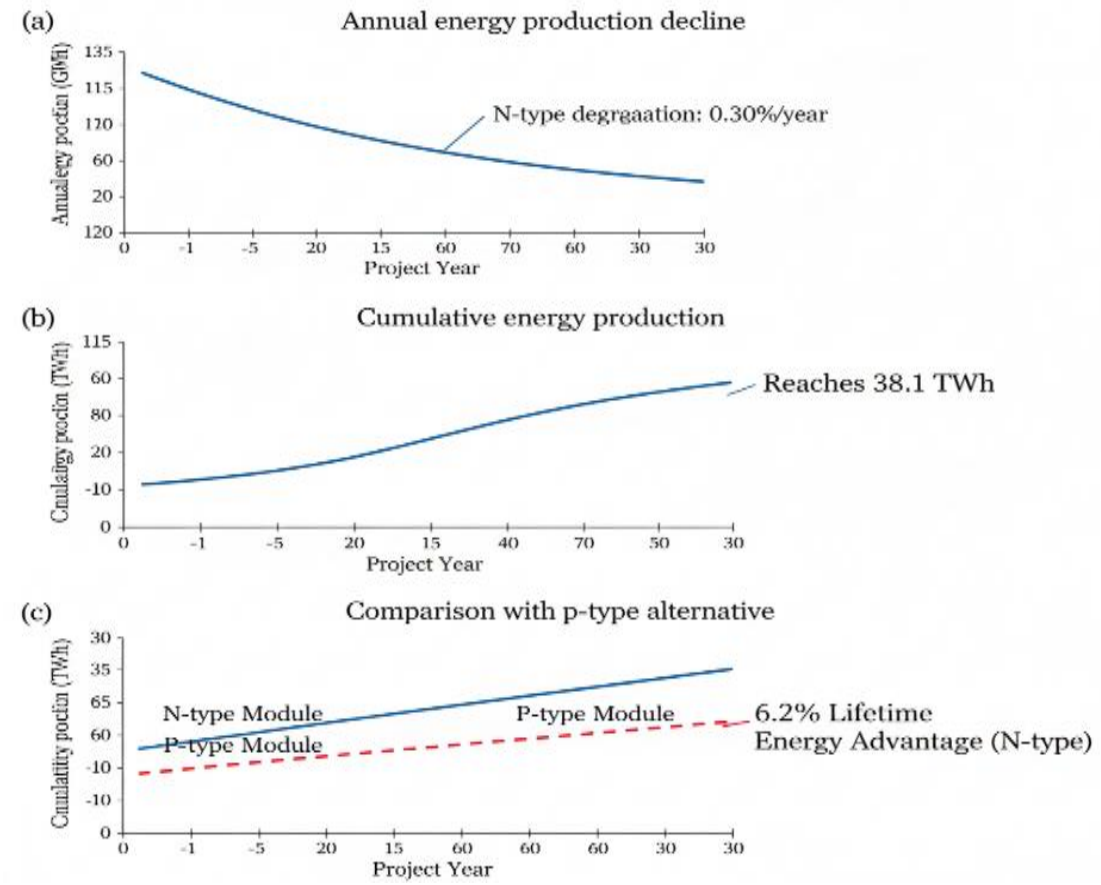

Figure 9: Long-term performance projection over a 30-year project lifetime

Risk Assessment and Mitigation

A risk assessment points out various types of risks that need to be managed in a project. Of these, political risks are the most challenging and include risks such as government instability, policy changes, failure to honor contracts, and security risks. To manage these risks, the strategy proposes political risk insurance through international organizations and export credit agencies of respective countries, international partnerships to share political risks, staged development to enable periodic risk reviews, and enhanced security for critical infrastructure.

Technical risks relate to the performance of the floating platform in practical conditions, the reliability of the platform over time in a severe marine environment, and the ability to integrate it with the power grid. These issues can be addressed by prototype testing and validation, comprehensive commissioning and performance validation, cautious design margins, and comprehensive grid impact studies with corresponding mitigation equipment.

Financial risks, particularly exchange rate fluctuations, payment defaults, and availability of low-cost financing, require hard currency revenue streams (possibly through export agreements), reserves and escrow accounts, blended financing that combines concessional and commercial funds, and partial risk guarantees from development finance institutions. Figure 10 illustrates the risk matrix for the project risks. The bubble size is proportional to the risk score, i.e., the product of the probability and impact of the risk. The bubble colors represent the risk types. The technical risks are blue in color, economic risks are green, political risks are red, environmental risks are yellow, and social risks are orange. The arrows indicate how effective the mitigation measures are, showing where they point.

CONCLUSIONS

This study demonstrates that a 600 MW solar power plant in a floating system off Al-Khoms, Libya, is technically viable and economically feasible as a renewable energy source, with great prospects for sustainable development. Based on a performance analysis modelled in PVsyst, taking into account the sea's special thermal characteristics, the study estimates that the solar power plant will produce an annual energy output of 1.35 TWh and a performance ratio of 82.3%. These results exceed those of conventional ground-mounted solar power plants, thanks to the superior cooling effects and the advantages of bifacial cells.

The technical advantages of floating solar power plants in Mediterranean regions are evident and measurable. The reduction of cell temperatures by 6-9°C increases energy production, and the project will conserve approximately 1.25 million cubic meters of water annually, which is an added economic and environmental benefit. The use of existing thermal power infrastructure for integration purposes provides technical synergies and economic advantages, further improving the project's economics.

Authors' Contributions: **Imbayah**: conceptualization and methodology and writing original draft preparation; **Nassar**, **El-Khozondar** and **Mohammed**: review editing and English proofreading; **Khaleel** and **Elmnifi**: formal analysis. All authors have read and agreed to the published version of the manuscript.

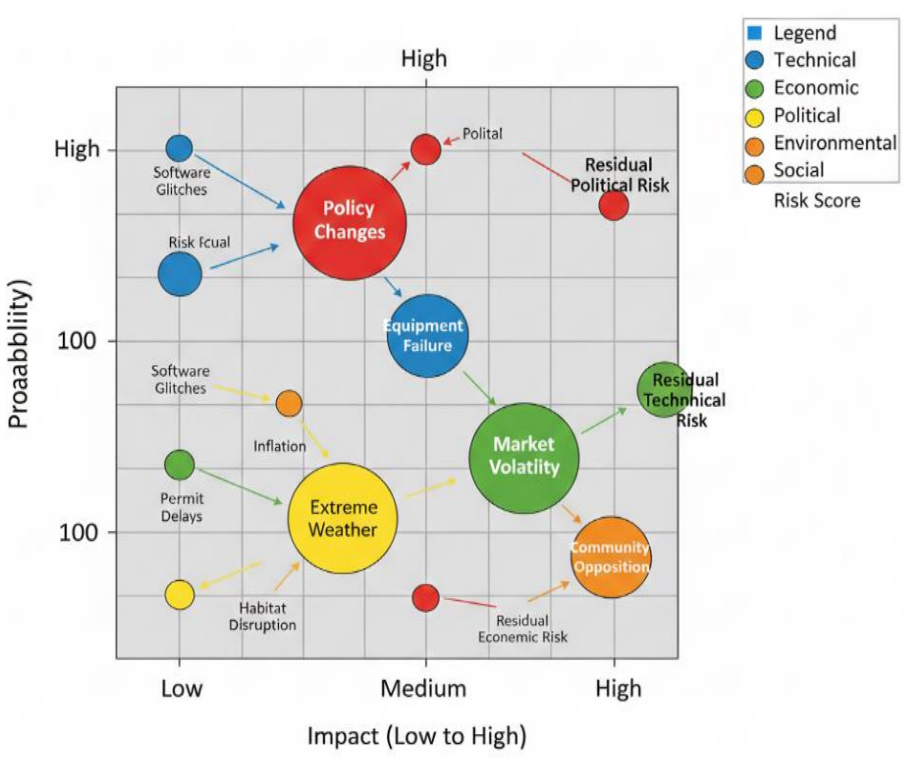

Figure 10: Risk matrix plot

Funding: "This research received no external funding."
Data Availability Statement: "The data are available at request."
Conflicts of Interest: "The authors declare no conflict of interest."

References

[1] N. Fathi, et al. "Assessing the Viability of Solar and Wind Energy Technologies in Semi-Arid and Arid Regions: A Case Study of Libya's Climatic Conditions." *Appl. Sol. Energy*, vol. 60, pp. 149–170, 2024. https://doi.org/10.3103/S0003701X24600218

[2] I. Imbayah, et al. "Design of a PV Solar-Covered Parking System for the College of Renewable Energy Tajoura, Libya: A PVsyst-Based Performance Analysis", *Univ Zawia J Eng Sci Technol*, vol. 3, no. 2, pp. 288–307, Dec. 2025. https://doi.org/https://doi.org/10.26629/uzjest.2025.23

[3] I. Latiwash, and A. Abubaker. "Performance Analysis and Sizing Optimization of a Utility Scale Stand-Alone Renewable Energy PV/Battery Storage System for Urban Zones." *University of Zawia Journal of Engineering Sciences and Technology*, vol. 3, no. 2, pp. 261–275, 2025. https://doi.org/10.26629/uzjest.2025.21

[4] A. Alkhazmi, et al. "Design and Analysis of PV Solar Street Lighting systems in Remote Areas: A Case Study." *Wadi Alshatti University Journal of Pure and Applied Sciences*, vol. 4, no. 1, pp. 1-14, 2026. https://doi.org/10.63318/waujpasv4i1_01

[5] M. Al-Maghalseh, A. Hammad, M. Hamdan, and E. Abdelhafez. "Thermal Comfort of Buildings Integrated Photovoltaics (BIPV)." *Wadi Alshatti University Journal of Pure and Applied Sciences*, vol. 4, no. 1, pp. 146-164, 2026. https://doi.org/10.63318/waujpasv4i1_16

[6] M. Ramadan, S. Khaled, and H. Ramadan. "Renewable energy resources and energy management in Libya: Future vision." *Journal of Renewable and Sustainable Energy*, vol. 10, no. 5, 2018. https://doi.org/10.1063/1.5049786

[7] A. Elmabruk, M. Salem, M., Khaleel, and A. Mansour. "Prediction of Wind Energy Potential in Tajoura and Mislata Cities." *Wadi Alshatti University Journal of Pure and Applied Sciences*, vol. 3, no. 2, pp. 125-131, 2025. https://doi.org/10.63318/waujpasv3i2_17

[8] S. Kumar, et al. "Floating photovoltaic systems: A carbon footprint analysis." *Renewable Energy*, vol. 142, pp. 233–241, 2019. https://doi.org/10.1016/j.renene.2019.05.100

[9] K. Anusuya, and K. Vijayakumar. "A comparative study of floating and ground-mounted photovoltaic power generation in Indian contexts," *Cleaner Energy Systems*, vol. 9, 2024, Art. no. 100140, https://doi.org/10.1016/j.cles.2024.100140

[10] N. Sahu, A. Chaturvedi, and S. Sharma. "A comprehensive review on exploration of eco-friendly energy generation from floating solar photovoltaic technologies." *Engineering Science and Technology, an International Journal*, vol. 40, p. 101389, 2023. https://doi.org/10.1016/j.jestch.2023.101389

[11] K. Sahu, M. Tiwari, and Y. Srivastava. "Performance enhancement of hybrid PV-TEG system through combined effect of radiative cooling and bifacial PV panel." *Energy Conversion and Management*, vol. 247, p. 114715, 2021. https://doi.org/10.1016/j.enconman.2021.114715

[12] M. Elnaggar, et al. "Technical and environmental cost-benefit analysis of strategies towards a green economy in the electricity sector in Libya," *Economics and Policy of Energy and the Environment*, pp. 133-167, Nov. 2025, https://doi.org/10.3280/EFE2025-002007

[13] Y. Nassar, A. Salem. "The reliability of the photovoltaic utilization in southern cities of Libya." Desalination, vol. 209, no. (1-3), pp. 86-90, 2007. https://doi.org/10.1016/j.desal.2007.04.013

[14] K. Amer, et al. "Thermoelectrical analysis of a new hybrid PV-thermal flat plate solar collector." In *8th International*

Engineering Conference on Renewable Energy & Sustainability (ieCRES), 2023

[15] M. Elmnifi, et al. "Design and manufacture of a photovoltaic thermal solar collector equipped with aluminum foam fins for enhanced electrical, thermal, and integrated performance." *International Communications in Heat and Mass Transfer*, vol. 173, p. 110844, 2026. https://doi.org/10.1016/j.icheatmasstransfer.2026.110844.

[16] D. King, W. Boyson, and J. Kratochvil. "Photovoltaic Array Performance Model." *Sandia National Laboratories*, SAND2004-3535, 2004. https://prod-ng.sandia.gov/techlib-noauth/access-control.cgi/2004/043535

[17] A. Golroodbari, et al. "Pooling the cable: A techno-economic feasibility study of integrating offshore floating photovoltaic solar technology within an offshore wind park." *Solar Energy*, vol. 219, pp. 705–716, 2021. https://doi.org/10.1016/j.solener.2020.12.062

[18] Y. Yong, et al. "Assessment of water quality and phytoplankton community structure of an on-shore floating photovoltaic system." *Environmental Monitoring and Assessment*, vol. 194, no. 10, 2022. https://doi.org/10.1007/s10661-022-10123-4

[19] M. Khan, and M. Zubair. "Performance assessment of bifacial PV modules under desert climatic conditions and comparison with monofacial PV modules: Experimental and modelling." *Energy*, vol. 239, p. 122111, 2022. https://doi.org/10.1016/j.energy.2021.122111

[20] R. Cazzaniga, et al. "Floating photovoltaic plants: Performance analysis and design solutions." *Renewable and Sustainable Energy Reviews*, vol. 81, pp. 1730–1741, 2018. https://doi.org/10.1016/j.rser.2017.05.269

[21] S. Tagliapietra. "Energy: A key variable in the Middle Eastern equation." *ISPI Commentary*, 2016. [Online]. https://www.ispionline.it

[22] International Monetary Fund, "Libya: 2022 Article IV Consultation." IMF Country Report No. 22/402, Dec. 2022. https://www.imf.org

[23] World Bank. *Libya Economic Monitor: Navigating Uncertainty*, World Bank Group, Washington, DC, 2021. Available: https://www.worldbank.org

[24] E. Almhdi, and G. Miskeen. "Power and Carbon Footprint Evaluation and Optimization in Transitioning Data Centres." *Wadi Alshatti University Journal of Pure and Applied Sciences*, vol. 3, no. 2, pp. 221-229, 2025. https://doi.org/10.63318/waujpasv3i2_28

[25] K. Amer, et al. "Economic-Environmental-Energetic (3E) analysis of Photovoltaic Solar Energy Systems: Case Study of Mechanical & Renewable Energy Engineering Departments at Wadi AlShatti University." *Wadi Alshatti University Journal of Pure and Applied Sciences*, vol. 3, no. 1, pp. 51-58, 2025. https://doi.org/10.63318/waujpasv3i1_09

[26] HJ El-Khozondar, et al. "Estimation of CO2 emission within Libya's electricity generation sector." *Next research*, vol. 2, no. 3, p. 100567, 2025. https://doi.org/10.1016/j.nexres.2025.100567

[27] K. Aissa, and S. Alsadi. "Estimation of Environmental Damage Costs from CO2e Emissions in Libya and the Revenue from Carbon Tax Implementation." *Low Carbon Economy*, vol. 8, pp. 118-132, 2017. https://doi.org/10.4236/lce.2017.84010

[28] A. Makhzom, et al. " Estimation of CO2 emission factor for Power Industry Sector in Libya." In *The 8th International Engineering Conference on Renewable Energy & Sustainability (ieCRES 2023)*, Gaza, Palestine, 08-09 May 2023. https://doi.org/10.1109/ieCRES57315.2023.10209528

[29] B. Ahmed, M. Hamdan, I. Imbayah, and A. Ahmed. "Technical, Economical and Environmental Aspects of Hybrid Renewable Energy Systems." *Scientific Journal for Publishing in Health Research and Technology*, vol. 1, no. 2, pp. 01-17, 2025. https://doi.org/10.65420/sjphrt.v1i2.8

[30] S. Mohammed, et al. "Carbon and Energy Life Cycle Analysis of Wind Energy Industry in Libya." *Solar Energy and Sustainable Development Journal*, vol. 12, no. 1, pp. 50–69, 2023. https://doi.org/10.51646/jsesd.v12i1.150

[31] IRENA. *Renewable Energy Outlook: Libya*, International Renewable Energy Agency, Abu Dhabi, 2021. https://www.irena.org

[32] A. Abdunnabi, and S. Ramadan. "Assessment of renewable energy system for electricity generation in Libya," *Journal of Renewable Energy*, vol. 2020, pp. 1–11, 2020. https://doi.org/10.1155/2020/1234567

[33] M. Kottek, J. Grieser, C. Beck, B. Rudolf, and F. Rubel. "World map of the Köppen-Geiger climate classification updated," *Meteorologische Zeitschrift*, vol. 15, no. 3, pp. 259–263, 2006. https://doi.org/10.1127/0941-2948/2006/0130

[34] N. Abohamoud, et al. "Regression Model for Optimum Solar Collectors' Tilt Angles in Libya." In *The 8th International Engineering Conference on Renewable Energy & Sustainability (ieCRES 2023)*, Gaza Strip, Palestine. https://doi.org/10.1109/ieCRES57315.2023.10209547

[35] N. Abuhamoud, et al. "Investigating the applicability of horizontal to tilted sky-diffuse solar irradiation transposition models for key Libyan cities." in IEEE 2nd International Maghreb Meeting of the Conference on Sciences and Techniques of Automatic Control and Computer Engineering (MI-STA). Sabratha-Libya, 2022. https://doi.org/10.1109/MI-STA54861.2022.9837500

[36] S. Alsadi, et al. "Determination of the Most Accurate Horizontal to Tilted Sky-Diffuse Solar Irradiation Transposition Model for the Capital Cities in MENA Region." In *Conference: 3rd International Conference on Smart Grid and Renewable Energy, Qatar- Doha*. 2022. https://www.researchgate.net/publication/361108750

[37] M. Khaleel, et al. "Sensitivity of global solar irradiance to transposition models: Assessing risks associated with model discrepancies." *e-Prime - Advances in Electrical Engineering, Electronics and Energy*, vol. 11, p. 100887, 2025. https://doi.org/10.1016/j.prime.2024.100887

[38] N. Fathi, A. Hafez, and S. Alsadi. "Multi-Factorial Comparison for 24 Distinct Transposition Models for Inclined Surface Solar Irradiance Computation in the State of Palestine: A Case Study." Front. Energy Res., vol. 7, p. 163, 2020. https://doi.org/10.3389/fenrg.2019.00163

[39] N. Fathi, S. Alsadi, K. Ali, A. Yousef, and M. Fakher. "Numerical Analysis and Optimization of Area Contribution of The PV Cells in the PV/T Flat-Plate Solar Air Heating Collector." *J. Solar Energy Res. Updat.*, vol. 6, pp. 43–50, 2019. https://doi.org/10.31875/2410-2199.2019.06.5

[40] A. Aqila, Y. Nassar, H. El-khozondar, and S. Suliman. "Design of hybrid renewable energy system (PV/wind/battery) under real climatic and operational conditions to meet full load of the residential sector: A case study of a house in Samno village– Southern region of Libya." *Wadi Alshatti Univ. J. Pure Appl. Sci.*, vol. 3, no. 1, pp. 186-181, 2025. https://doi.org/10.63318/waujpasv3i1_23

[41] E. Salim, et al. "A Brief Overview of Hybrid Renewable Energy Systems and Analysis of Integration of Isolated Hybrid PV Solar System with Pumped Hydropower Storage

for Brack city - Libya." *Wadi Alshatti University Journal of Pure and Applied Sciences*, vol. 3, no. 1, pp. 152-167, 2025. https://doi.org/10.63318/waujpasv3i1_22

[42] H. El-Khozondar, et al. "Sustainable street lighting in Gaza: Solar energy solutions for main street." *Energy 360*, vol. 4, no. 12, p. 100042, 2025. https://doi.org/10.1016/j.energ.2025.100042

[43] H. El-Khozondar, et al. "Photovoltaic Solar Energy for Street Lighting: A Case Study at Kuwaiti Roundabout, Gaza Strip, Palestine." *Power Engineering and Engineering Thermophysics*, vol. 3, no. 2, pp. 77–91, 2024. https://doi.org/10.56578/peet030201

[44] D. Albuzia, A. Ali, M. Mohmed, and A. Hafez. "Reliable and Robust Optimal Interleaved Boost Converter Interfacing PhotoVoltaic Generator." *Wadi Alshatti University Journal of Pure and Applied Sciences*, vol. 3, no. 2, pp. 192-201, 2025. https://doi.org/10.63318/waujpasv3i2_24

[45] A. Al-Mathnani, A. Mohammed, S. Al-Hashmi, and E. Geepalla. "Control and Modification of 12-Pulse Static Compensator with PV Cell Using New Control Algorithm." *Wadi Alshatti University Journal of Pure and Applied Sciences*, vol. 3, no. 1, pp. 30-34, 2025. https://doi.org/10.63318/waujpasv3i1_06

[46] J. Remund, et al. *Meteonorm Handbook Part II: Theory*, Meteotest, Bern, Switzerland, 2020. https://meteonorm.com

[47] M. Šúri, T. Cebecauer, and A. Skoczek. "Solargis: Solar data and online applications for PV planning and performance assessment." in *Proc. 26th European Photovoltaic Solar Energy Conf. and Exhibition*, Hamburg, Germany, 2011, pp. 4749–4753

[48] A. Mermoud, and B. Wittmer. "PVsyst 7, a tool for the study and simulation of photovoltaic systems." University of Geneva / PVsyst SA, 2023. https://www.pvsyst.com

[49] K. McIntosh, et al. "Bifacial photovoltaic module technology." in *Handbook of Photovoltaic Science and Engineering*, 3rd ed., Wiley, 2023, ch. 28. https://doi.org/10.1002/9781119801928.ch28

[50] B. Burger, and D. Kranzer. "Extreme high efficiency PV power converters." in *Proc. 13th European Conf. Power Electronics and Applications*, Barcelona, Spain, pp. 1–13, 2009.

[51] J. Abella, et al. "Thermodynamic modeling and parametric study of a solar assisted heat pump." *Applied Thermal Engineering*, vol. 140, pp. 11–24, 2018. https://doi.org/10.1016/j.applthermaleng.2018.04.123

[52] C. Chin, et al. "Temperature cell modelling of floating solar farm." *Energy Procedia*, vol. 143, pp. 382–387, 2017. https://doi.org/10.1016/j.egypro.2017.12.555

[53] M. Mohammed, E. Mohammed, and R. Elzer. "Techno-Economic Feasibility of Parabolic Trough Solar Steam for Thermal Enhanced Oil Recovery." *Wadi Alshatti University Journal of Pure and Applied Sciences*, vol. 4, no. 1, pp. 184-190, 2026. https://doi.org/10.63318/ waujpasv4i1_19

[54] H. El-Khozondar, et al. "Economic and environmental implications of solar energy street lighting in urban regions: A case study." *Wadi Alshatti Univ. J. Pure Appl. Sci.*, pp. 142–151, 2025, https://doi.org/10.63318/waujpasv3i1_21

[55] Y. Fathi, et al. "Estimation of CO2 emission within Libya's electricity generation sector." *Next Res.*, 2025, https://doi.org/10.1016/j.nexres.2025.100567

[56] A. Alfathi, G. Miskeen, and W. Mremi. "Evaluation and Prediction Performance of Solar Panel and Wind Turbine Systems Using Simulation." *Wadi Alshatti University Journal of Pure and Applied Sciences*, vol. 4, no. 1, pp. 94-104, 2026. https://doi.org/10.63318/waujpasv4i1_10

[57] M. Inweer and Y. Nassar. "Carbon emissions life cycle assessment of cement industry in Libya," *Wadi Alshatti Univ. J. Pure Appl. Sci.*, vol. 3, no. 2, pp. 162–173, 2025, https://doi.org/10.63318/waujpasv3i2_21

[58] M. Inweer, et al. "Carbon footprint life cycle assessment of cement industry in Libya." *Discov. Concr. Cem.*, vol. 1, no. 37, 2025. https://doi.org/10.1007/s44416-025-00037-1

[59] B. Ahmed, H. El-Khozondar, and M. Khaleel. "Optimal Design of Hybrid Renewable Energy System (PV/Wind/PHS) Under Multiple Constraints of Connection to the Electricity Grid: A Case Study." *Wadi Alshatti University Journal of Pure and Applied Sciences*, vol. 4, no. 1, pp. 83-93, 2026. https://doi.org/10.63318/waujpasv4i1_09

[60] A. Abduallah, S. Mohammed, and M. Ghatus. Integrating Electricity Sub-Grid with Pumped Hydropower Storage System for Grid Stability and Sustainability. *Wadi Alshatti University Journal of Pure and Applied Sciences*, vol. 3, no. 2, pp. 322-332, 2025. https://doi.org/10.63318/waujpasv3i2_40

[61] M. Al-Maghalseh. "The environmental impact and societal conditions of PV power plants: A case study of Jericho Gate-Palestine state," *Wadi Alshatti Univ. J. Pure Appl. Sci.*, vol. 3, no. 2, pp. 16–31, 2025, https://doi.org/10.63318/waujpasv3i2_03

[62] A. Amhimmid, et al. "Financial modeling of social and environmental impacts of wind farm in urban zones: A case study of Zawia-Libya." *Int. J. Energy Environ. Eng.*, vol. 15, no. 4, 2024. https://doi.org/10.57647/ijeee.2024.1504.17.

[63] K. Moumani. "Management of sustainable development in the light of Arab and international cooperation, a case study of the Arab vision of management of sustainable development." *Wadi Alshatti University Journal of Pure and Applied Sciences*, vol. 1, no 1, pp. 1-8, 2023. https://doi.org/10.63318/waujpasv1i1_01

[64] M. Abdunnabi, et al. "Energy savings strategy for the residential sector in Libya and its impacts on the global environment and the nation economy ." Advances in Building Energy Research, vol. 17, no. 4, pp. 379-411, 2023. https://doi.org/10.1080/17512549.2023.2209094